

Correlations between the Viscoelastic Behavior of Pyrene-Labeled Associative Polymers and the Associations of Their Fluorescent Hydrophobes

Telmo J. V. Prazeres and Jean Duhamel*

*Institute for Polymer Research, Department of Chemistry, University of Waterloo,
Waterloo, ON N2L 3G1, Canada*

Keith Olesen and Greg Shay

The Dow Chemical Company, UCAR Emulsion System, 410 Gregson Drive, Cary, North Carolina 27511

Received: May 3, 2005; In Final Form: June 11, 2005

The viscoelastic behavior of a series of three pyrene-labeled hydrophobically modified alkali swellable emulsion copolymers (Py–HASEs) was investigated. All Py–HASEs thickened the aqueous solutions with viscosities orders of magnitude larger than that of a HASE control which displayed no pyrene hydrophobe. This fact demonstrated that the pyrene molecule is a good hydrophobe for associative thickeners such as HASEs. The Py–HASE solutions exhibited shear thinning, whose magnitude was found to increase with increasing pyrene content. A large shear-thinning effect indicates that a large fraction of the elastically active cross-links has been severed. Fluorescence measurements on the Py–HASEs confirmed that the smaller the pyrene content of the Py–HASE, the more intermolecular associations it formed, in agreement with the results obtained by rheology. Above the overlap concentration of the polymers, the zero-shear viscosity of the Py–HASE solutions increased steeply with increasing polymer concentration. The onset concentration where viscosity increases matches the onset concentration where intermolecular associations are being formed, as probed by fluorescence. Oscillatory rheological measurements were carried out to determine the terminal relaxation time, T_d , and the storage modulus at the infinite time limit, G_0 , of the Py–HASE network. G_0 was found to increase with decreasing pyrene contents, indicating that Py–HASEs with lower pyrene contents exhibited a higher density of elastically active chains. This result is in agreement with the trends obtained by the fluorescence and steady-state rheology measurements. A model is suggested that accounts for the fluorescence and rheology results.

Introduction

In aqueous solutions, the hydrophobic groups of water-soluble associating polymers (APs) tend to associate intra- and intermolecularly into micelle-like aggregates.¹ These aggregates form the keystones of an interpolymeric network which leads to a dramatic enhancement of the solution viscosity. The “fluidity” of the chains taking part in these physical networks has been described as being the most striking aspect of the viscoelastic behavior of AP solutions.² Since the chains are connected to one another via transient junctions, each chain has the possibility to flow through the entire network as successive sections of the chain are freed from the macroscopic network when a hydrophobic group unties itself from a cross-linking center. For gel-forming AP solutions, the local fluidity of the chains observed at the molecular level stands in sharp contrast with the overall immobility of the AP solution which does not flow at low shear.

Transient networks formed by hydrophobically modified ethoxylated urethanes (HEURs), a well-known AP, follow a Maxwellian behavior with a single characteristic relaxation time which has been attributed to the residence time, τ_{RES} , of a hydrophobic group inside a hydrophobic aggregate.^{3,4} In the case of transient networks formed by APs with hydrophobes randomly distributed along the backbone, a much more complicated

dynamic behavior is usually observed which cannot be described by the Maxwell model.^{5–18} Hydrophobically modified polyacrylamides (HMPAMs) with short hydrophobic blocky structures or “stickers” distributed along the backbone exhibit such a complex viscoelastic behavior^{5,6} which can be explained by the “sticky reptation” model introduced by Leibler et al.¹⁹ In this model, the distance between entanglements is shorter than that between the stickers and the HMPAM chains form an entangled transient network. The model predicts two relaxation times for a network held by cross-linking centers formed by a “multisticker” chain. The short relaxation time corresponds to τ_{RES} , while the long one is the terminal relaxation time, T_d , which is the time taken by a chain to “reptate” outside its tube.²⁰ T_d depends on the chain length, the number of stickers per chain, τ_{RES} , and the fraction of associated stickers. Interestingly, the models which were developed for telechelic APs such as HEURs and multisticker APs such as HMPAMs do not explain the viscoelastic properties of other APs such as hydrophobically modified alkali swellable emulsion copolymers (HASEs).^{7–15} Nevertheless, this lack of understanding has not prevented HASEs to become widely used as viscosity modifiers in paints, paper coatings, and glycol-based aircraft anti-icing fluids.^{9,21}

As shown in Figure 1, HASEs are terpolymers made of ~50 mol % methacrylic acid, ~50 mol % ethyl acetate, and a few mol % of a hydrophobically modified macromonomer (HMM).¹³ The HMM consists of a poly(ethylene oxide) (PEO) spacer

* To whom correspondence should be addressed.

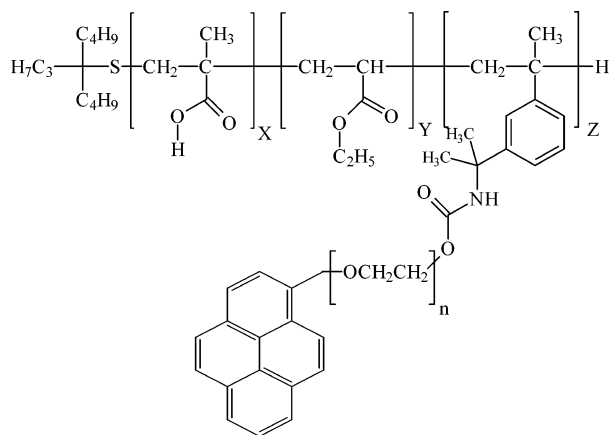


Figure 1. Chemical structure of Py–HASE. The molar fractions *X*, *Y*, and *Z* of HASE0, HASE12, HASE35, and HASE48 are listed in Table 1. The degree of ethoxylation, *n*, equals 53.

joined at one end to a methylstyrene via a urethane function and to a hydrophobe via an ether bond at the other end. In basic aqueous solutions, the HASE backbone is a negatively charged polyelectrolyte and the hydrophobes at the ends of the PEO spacers induce the formation of intermolecular hydrophobic aggregates which are responsible for the peculiar viscoelastic properties of HASE solutions. The viscoelastic behavior of aqueous solutions of HASEs is complicated, as it exhibits multiple relaxation times.^{12,14} This is different from the characteristic single relaxation time exhibited by HEURs for which the disengagement of a hydrophobe from a cross-linking center represents a significant disruption of the polymeric network. In the case of multisticker chains such as HASEs, the disengagement of a hydrophobe from a hydrophobic aggregate does not disrupt the network as much, because the other hydrophobes of the chain are still linked to other cross-linking centers which hold the main chain in place, delaying its diffusion.

In view of the important role played by the hydrophobes toward conferring the interesting viscoelastic properties displayed by any AP solution, numerous efforts have been devoted to probing the behavior of these hydrophobes in solution. One particularly effective approach substitutes fluorescent chromophores in lieu of the hydrophobes.^{22,23} If the chromophores are chosen so that their fluorescence changes upon aggregation, information about the level of association of the chromophores can be obtained. Pyrene is such a chromophore which, upon excitation by UV light, emits in the blue (~375 nm) as a monomer but emits in the green (~480 nm) as an aggregate.²⁴ Several studies have demonstrated that analysis of the monomer and excimer fluorescence decays of pyrene attached onto a polymer backbone yields the fraction of aggregated pyrenes.^{25–31} In particular, such experiments have been performed on a series of pyrene-labeled hydrophobically modified alkali swellable emulsion copolymers (Py–HASEs) where the traditional aliphatic hydrophobe of HASEs was replaced by pyrene.²⁵ The interactions of Py–HASE with surfactants were also probed, and the fraction of aggregated pyrenes of a Py–HASE molecule was found to decrease as the surfactant sodium dodecyl sulfate was added to the Py–HASE solution.^{26,27}

Following these fluorescence experiments, it remained to be seen to what extent the viscoelastic properties of Py–HASEs would mimic those displayed by commercial nonfluorescent HASEs and, even more importantly, whether the combination of fluorescence and rheological data could shed new light on the role of the hydrophobes in inducing the intriguing viscoelastic properties of HASEs. These questions have been addressed

TABLE 1: Molar Fractions of Methacrylic Acid, *X*, Ethyl Acrylate, *Y*, and Hydrophobically Modified Macromonomer, *Z*, for the HASE Latexes

| sample | <i>X</i> | <i>Y</i> | <i>Z</i> |
|--------|----------|----------|----------|
| HASE48 | 0.50 | 0.49 | 0.011 |
| HASE35 | 0.45 | 0.55 | 0.006 |
| HASE12 | 0.40 | 0.59 | 0.002 |
| HASE0 | 0.40 | 0.59 | 0.002 |

in the present manuscript which includes an extensive characterization of the rheological properties of Py–HASEs.

Experimental Section

All chemicals and instruments used in this work were described in an earlier publication.²⁵ The structure of Py–HASE is shown in Figure 1. The pyrene content of the Py–HASE samples equals 0, 12, 35, and 48 μmol/g, and these polymers are referred to as HASE0, HASE12, HASE35, and HASE48, respectively. The four HASE samples were prepared by DOW. Their molar fractions of methacrylic acid, *X*, ethyl acrylate, *Y*, and hydrophobically modified macromonomer (HMM), *Z*, are listed in Table 1. The pyrene-labeled HMM has been fully characterized in an earlier publication.³²

The molecular weight of HASE polymers is notoriously difficult to estimate due to their inherent tendency to aggregate in water and their poor solubility in organic solvents.^{8,33} To the best of our knowledge, the only careful study of the molecular weight of nonaggregated HASEs was done at DOW (then Union Carbide) by entrapping the hydrophobes of the copolymer with a cyclodextrin and using light scattering to determine the weight average molecular weight, *M_w*, the radius of gyration, and the hydrodynamic radius of the polymers.³³ This work led to the conclusion that the emulsion polymerization used by DOW produces HASE copolymers exhibiting little branching and *M_w* around $(1–2) \times 10^5$ g/mol. In the present study, the Py–HASE samples were produced by DOW using the same procedure used to synthesize other nonfluorescent HASEs, such as that in ref 33. They are expected to exhibit similar features in terms of *M_w* ($\sim(1–2) \times 10^5$ g/mol) and a low level of branching.

The HMM of HASE0 was synthesized by initiating the anionic polymerization of the PEO spacer with methanol instead of 1-pyrenemethanol for the HMM of HASE12, HASE35, and HASE48. The only instrument not presented in the earlier publication²⁵ is the rheometer which is described hereafter.

Rheology. Rheology measurements were carried out on a stress-controlled Paar Physica DSR 4000 rheometer interfaced with a UDS 200 tower. For concentrated solutions (viscosities higher than 200 Pa·s), a parallel-plate geometry with a 25 mm diameter plate was used. For solutions with viscosities below 200 Pa·s, the bob and cup geometry was used. The bob consists of a concentric cylinder 45 mm in diameter with a 24° cone-shaped bottom. All experiments were performed at room temperature (23 ± 1 °C). All data points were taken within the sensitivity range of the instrument according to the specifications provided by the manufacturer. The stress values used for the angular frequency sweeps were within the linear viscoelastic regime, where the values of *G'* and *G''* remain constant upon varying the stress applied. The angular frequency interval used in this work ranged from 0.001 to 100 rad·s^{−1}. Different frequency intervals were used for different samples to ensure that their viscoelastic response remained within the sensitivity of the instrument, as described in the Paar Physica DSR 4000 manual. The steady-shear viscosity (flow) measurements were performed to obtain the zero-shear viscosities and to probe the thinning effect of Py–HASEs as a function of pyrene content

and polymer concentration. The broadest shear rate interval used ranged from 0.0001 to 1000 s^{-1} .

Sample Preparation. In an earlier publication,²⁵ the fluorescence experiments performed on the Py–HASE solutions were carried out in either water at pH 9 or a 0.05 KCl aqueous solution at pH 9, where the pH of the solution was controlled by adding minute amounts of concentrated NaOH or HCl solution. During this first set of experiments, the pH was observed to decrease over time, certainly due to the dissolution of atmospheric CO_2 into the aqueous solutions. The early fluorescence experiments were carried out over a few days during which the pH did not have time to drift much.²⁵ However, pH stability became a serious issue for the rheology experiments carried out in this work where HASE aqueous solutions were kept aerated for a period of weeks. Consequently, the procedure for the preparation of the aqueous stock solutions used in this study needed to be modified. When NaOH was used as the base to neutralize the polymer solution, some alterations of the sample could be observed after 4–5 days such as in the pH of the solutions, the relative intensities of the fluorescence of the pyrene monomer and excimer, and the rheological properties of the HASE solutions. In a paper by Tirtaatmadja et al.,³⁴ rheology was used to show that the use of NaOH as the base induces the degradation of HASEs. The degradation is thought to occur via the hydrolysis of the urethane groups over time. Hydrolysis of the ester group of the EA monomer can also occur, increasing the number of acid groups on the polymer backbone.

A stability study of the HASE solutions was performed. Several bases were used, and their effect on the fluorescence of HASE solutions was monitored over time. A carbonate aqueous solution was found to preserve the properties of HASE solutions for more than 7 weeks. Consequently, the HASE aqueous solutions used in this study were prepared with an aqueous solution of 0.01 M Na_2CO_3 and 0.05 M KCl at pH 9. The pH was adjusted to pH 9 by using a few drops of 1 M HCl or 0.5 M Na_2CO_3 solutions. The stability of the solutions was verified regularly with a pH meter and by steady-state fluorescence.

Results

The general chemical structure of Py–HASEs has been shown in Figure 1 where the terminal hydrophobe of the macromonomer is replaced by the fluorescent probe pyrene. Pyrene was selected to take advantage of its excimer-forming ability to monitor the process of association occurring between pyrene groups at the molecular level using fluorescence. It was shown in an earlier publication that the excimer in aqueous solution forms essentially via preassociated pyrenes with a small contribution of excimer being formed via diffusion.²⁵ Indeed, the fraction of pyrenes forming excimer via diffusion, f_{diff} , was found to range between 0.14 and 0.27 depending on the pyrene content and the concentration of the Py–HASE solution. By contrast, in a solvent like THF where the pyrene pendants are soluble, the excimer was formed mostly via diffusion and f_{diff} took a value between 0.83 and 0.93 depending on the pyrene content of the Py–HASE.²⁵ In aqueous solution, analysis of the pyrene monomer and excimer decays yielded a fraction of aggregated pyrenes equal to 0.58 ± 0.09 .²⁵ This meant that 58% of all pyrenes are associated in dilute solutions and in the early semidilute regime, that is, slightly above the overlap concentration, C^* . In the present study, solutions of HASEs having pyrene contents of 0, 12, 35, and 48 $\mu\text{mol/g}$ referred to as HASE0, HASE12, HASE35, and HASE48, respectively, were investigated in aqueous solutions (pH 9, 0.05 M KCl, 0.01 M Na_2CO_3) at polymer concentrations smaller and larger than C^* by fluorescence and rheology measurements. C^* was estimated from the inverse of the intrinsic viscosity, $[\eta]$, which was measured with an Ubbelohde viscometer.⁵ The $[\eta]$ values are listed in Table 2 and are discussed later on.

TABLE 2: Intrinsic Viscosities, $[\eta]$, and Critical Concentration, C^* , Obtained from Figure 4 for the HASE Polymers in Aqueous Solutions (pH 9, 0.05 M KCl, 0.01 M Na_2CO_3)

| | HASE0 | HASE12 | HASE35 | HASE48 |
|------------------------------|-------|--------|--------|--------|
| $[\eta]$, L/g | 0.53 | 0.42 | 0.30 | 0.10 |
| $[\eta]^{-1} \sim C^*$, g/L | 1.9 | 2.4 | 3.3 | 10.0 |
| C^* , g/L | | 1.8 | 5.5 | 13.4 |

Since pyrene has never been used as a hydrophobe for HASEs, it was important to characterize its role, if any, in the rheological behavior of HASEs. To this effect, HASE0 was synthesized where the hydrophobe is a methyl group. The viscoelastic behavior of aqueous solutions of HASE0 was determined and compared to that of the Py–HASEs. The aqueous solutions of HASEs were prepared as described in the Experimental Section. Figure 2 shows the variation of the steady-shear viscosity with shear rate for aqueous solutions of HASE0, HASE12, HASE35, and HASE48 at a concentration of 45 g/L in the semidilute regime. A small Newtonian regime is observed for all polymers at low shear rates where the viscosity is constant with shear rate. The viscosity value in this region is referred to as the zero-shear viscosity, η_0 . The viscosity profiles shown in Figure 2 demonstrate that pyrene is a very efficient hydrophobe since η_0 for all Py–HASEs is orders of magnitude larger than that of HASE0. The zero-shear viscosities of aqueous solutions of HASE0, HASE12, HASE35, and HASE48 at 45 g/L are respectively 0.9, 61, 2730, and 6240 Pa·s. The zero-shear viscosity values of aqueous solutions of all Py–HASEs are much higher than that for HASE0. This effect is similar to that observed for HASEs bearing other hydrophobes such as alkyl chains^{7,8,11} or nonylphenols.¹³ As for other hydrophobes, the trends shown in Figure 2 suggest that pyrene hydrophobicity plays a major role in enhancing the solution viscosity. Furthermore, increasing the pyrene content of the HASE samples resulted in a dramatic increase of the zero-shear viscosity of the solution. Intuitively, this behavior would suggest that increasing the pyrene density in the polymeric coils promotes more interpolymeric associations and a higher density of cross-linking centers, hindering the diffusion of the chains at the molecular level and resulting in stronger network

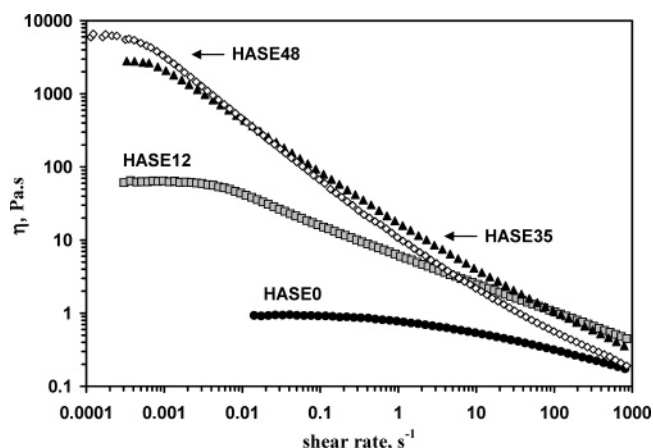


Figure 2. Steady-shear viscosity as a function of shear rate for HASEs in basic aqueous solutions (pH 9, 0.05 M KCl, 0.01 M Na_2CO_3) at 45 g/L.

formation. However, additional evidence obtained by the fluorescence and rheology measurements presented hereafter leads to the conclusion that increasing the pyrene content leads to a decrease of the number of intermolecular associations and to a dramatic increase in the terminal relaxation time of the Py-HASE network.

When stress is applied to the HASE solutions by increasing the shear rate, the intermolecular associations are severed and the viscosity drops. This effect, called shear thinning, occurs when $\log \eta$ decreases linearly with $\log \dot{\gamma}$. In Figure 2, the slopes of these straight lines are -0.40 , -0.65 , and -0.72 for HASE12, HASE35, and HASE48, respectively. Shear thinning is usually assumed to result from a transition where intermolecular associations are severed and the free hydrophobes rearrange to form intramolecular associations. The profiles shown in Figure 2 suggest that this transition occurs more easily with HASEs having higher pyrene contents because the onset shear rate, where shear thinning occurs, decreases with increasing pyrene content (5×10^{-3} , 0.8×10^{-3} , and $0.3 \times 10^{-3} \text{ s}^{-1}$ for HASE12, HASE35, and HASE48, respectively) and because the slopes corresponding to shear thinning in Figure 2 increase with increasing pyrene content.

To better understand the role of pyrene and the effect of pyrene content on the steady-shear viscosity of HASEs, a concentration study was performed. Figure 3 shows representative steady-shear viscosity profiles of aqueous solutions of HASE0, HASE12, and HASE48. The zero-shear viscosities were obtained by averaging the values of the viscosity in the Newtonian plateau, and these values are plotted as a function of polymer concentration in Figure 4. HASE0 behaves very differently from Py-HASEs. The zero-shear viscosity increases with polymer concentration, C , according to a $C^{1.9}$ power law. The behavior of Py-HASEs is more complicated. At dilute concentrations, the viscosity is very low and increases only slightly with HASE concentration. Above a critical concentration, C_η , the viscosity increases dramatically with concentration. The higher the pyrene content of a given HASE, the more pronounced the viscosity increase is. The zero-shear viscosity of the aqueous HASE solutions increases with HASE concentration, C , according to a C^x power law where x equals 3.5 ± 0.0 , 8.0 ± 0.3 , and 12.8 ± 0.4 for HASE12, HASE35, and HASE48, respectively. The exponential increase of zero-shear viscosity with concentration for HASE35 and HASE48 is unusually steep, as has already been observed for other HASEs⁹ and comb polymers having a structure similar to that of HASEs.¹⁶ These results show that the thickening ability of the pyrene-labeled HASEs is at least comparable to and sometimes better than that of some nonfluorescent HASEs for which a smaller C^8 increase of η_0 was reported.⁹ At high concentration, η_0 in Figure 4 exhibits a slight downturn very similar to what has been reported in other studies of nonfluorescent HASEs.⁹

The trends reported in Figure 4 can be interpreted as follows. In very dilute solutions, the polymer coils do not interact with each other and only intramolecular interactions are expected to occur between the pyrenes. As the concentration increases, the coils associate to form clusters and the number of intermolecular associations between pyrenes increases. At C_η , the intermolecular associations become dominant, giving rise to the formation of a physical network in solution which results in the tremendous increase of the solution viscosity.

For nonassociative polymers, C_η is also the overlap concentration, C^* , above which the viscosity of polymer solutions increases sharply with concentration due to topological entanglements. The overlap concentration is usually estimated from

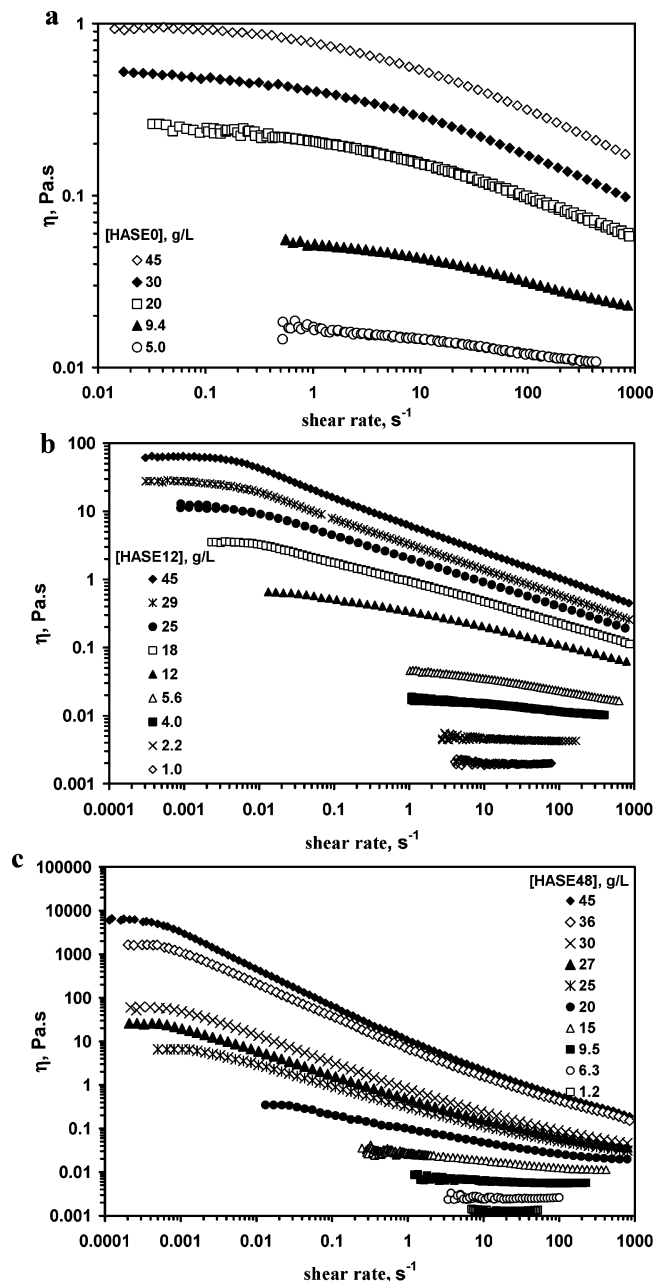


Figure 3. Representative profiles of the steady-shear viscosity as a function of shear rate for HASEs in basic aqueous solutions (pH 9, 0.05 M KCl, 0.01 M Na_2CO_3) at several HASE concentrations: HASE0 (a); HASE12 (b); HASE48 (c).

the intrinsic viscosity, $[\eta]$, according to the following relationship: $C^* \sim [\eta]^{-1.5}$. The value of C_η was determined for all HASEs as the intercept between the straight lines shown in the inset of Figure 4 and a horizontal line corresponding to the viscosity of water taken to equal 1.0 mPa.s. The intrinsic viscosities of all polymers were measured with an Ubbelohde viscometer. It is worth noting that all aqueous solutions contained 0.05 M KCl which screens the electrostatic interactions of the polyelectrolytes. The values of $[\eta]$, C^* , and C_η are listed in Table 2. The trends obtained between $[\eta]^{-1}$ and C_η agree rather well, giving credence to the fact that the onset of the viscosity increase given by C_η coincides with the onset of entanglement formation given by $[\eta]^{-1} \sim C^*$. This result leads to the conclusion that C^* and C_η are equivalent for the Py-HASE solutions. Furthermore, $[\eta]$ is found to increase with decreasing pyrene content (cf. Table 2). The compactness of

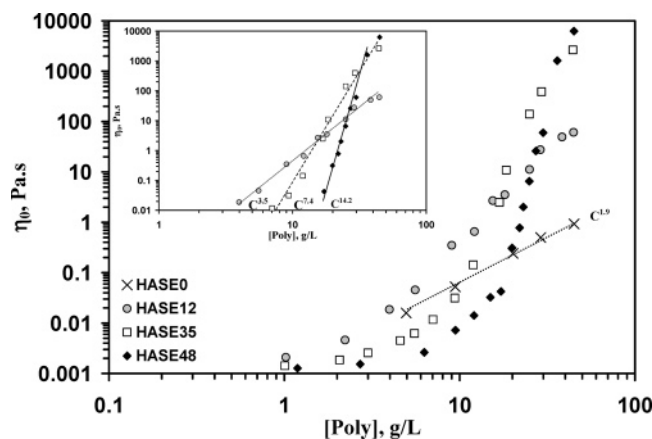


Figure 4. Concentration dependence of the zero-shear viscosity of HASEs in basic aqueous solutions (pH 9, 0.05 M KCl, 0.01 M Na₂CO₃). Inset: Concentration dependence of the zero-shear viscosity of HASEs in basic aqueous solutions (pH 9, 0.05 M KCl, 0.01 M Na₂CO₃) in the semidilute regime, i.e., above C^* .

the Py–HASE polymer coil is expected to increase with increasing pyrene content. It is often reported for APs that a higher hydrophobe content induces stronger intramolecular hydrophobic aggregation which shrinks the overall dimension of the polymer coil, so that the overlap concentration of an AP is larger than that of the unmodified polymer.^{35,36}

It must be noted that $[\eta]$ is very unlikely to represent the properties of individual Py–HASE chains. More realistically, polymeric aggregates made of a few Py–HASEs are present in solution at low polymer concentrations and the $[\eta]$ values listed in Table 2 report on the behavior of these Py–HASE aggregates.^{37,38} These polymeric aggregates are held together via the hydrophobic parts of the Py–HASEs, namely, hydrophobic stretches of ethylacrylate monomers and pyrene pendants. At the low polymer concentrations where the $[\eta]$ measurements were conducted, no interaggregate interactions are taking place, as demonstrated by the steady-state fluorescence measurements shown later.

Several facts have been established about the Py–HASEs in aqueous solutions in an earlier publication,²⁵ and they are briefly reviewed hereafter. The charges along the Py–HASE backbone extend the polymer coil, isolating the pyrene moieties, which reduces excimer formation by diffusion. In aqueous solutions, excimers are essentially generated via ground-state hydrophobic associations between pyrene moieties. Increasing the pyrene content of the HASEs promotes the formation of more nondiffusional excimer. The I_E/I_M values remained constant in aqueous solutions for the concentrations studied ranging from 0.02 g/L up to about 10–20 g/L.

In the present study, an alternative sample preparation protocol described in the Experimental Section was used to prepare more concentrated HASE solutions. Steady-state fluorescence spectra of the Py–HASEs were acquired for polymer concentrations ranging from 0.4 g/L up to 54 g/L. The I_E/I_M ratios were determined and are plotted as a function of the HASE concentration in a semilog plot in Figure 5. At lower concentrations, the values of I_E/I_M are constant, taking an average value of 0.03 ± 0.00 , 0.10 ± 0.00 , and 0.22 ± 0.01 for HASE12, HASE35, and HASE48, respectively. Constant I_E/I_M ratios at low polymer concentration were also obtained earlier,²⁵ and they suggest that excimer formation occurs intramolecularly at low polymer concentrations. The increase of the I_E/I_M ratios with increasing pyrene content follow the trend described in ref 25. Interestingly, the I_E/I_M ratio increases with concentration for

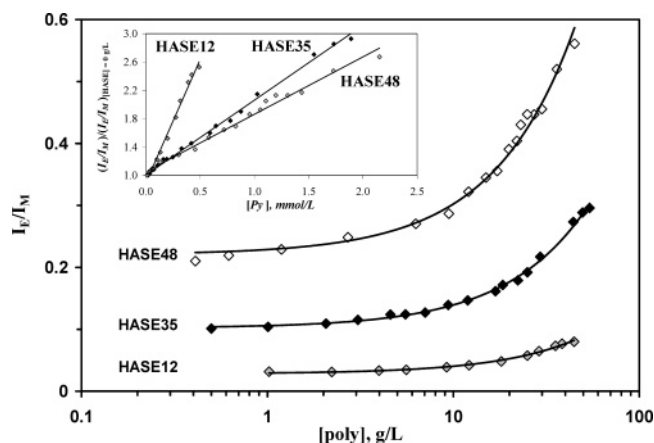


Figure 5. I_E/I_M ratios as a function of polymer concentration for basic aqueous solutions (pH 9, 0.05 M KCl, 0.01 M Na₂CO₃) of HASEs. Inset: $(I_E/I_M)/(I_E/I_M)_{([Py]=0\text{ g/L})}$ as a function of Py–HASE concentration.

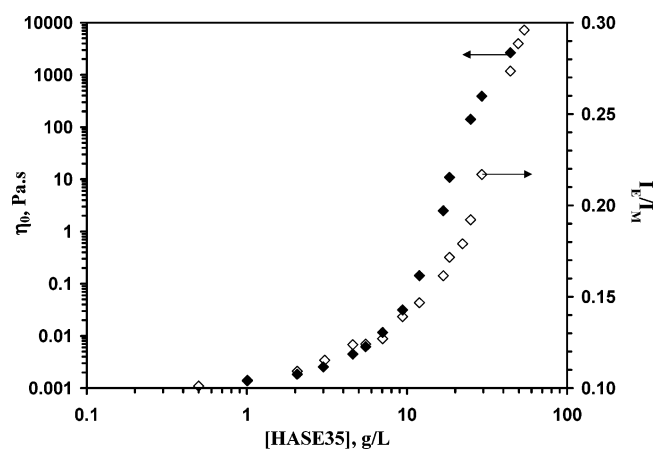


Figure 6. Zero-shear viscosity and I_E/I_M ratios as a function of polymer concentration for HASE35 in basic aqueous solutions (pH 9, 0.05 M KCl, 0.01 M Na₂CO₃).

all Py–HASEs (cf. Figure 5) in the same concentration region where the zero-shear viscosity starts to increase dramatically (cf. Figure 4). Such a behavior where the I_E/I_M ratio remains constant at low polymer concentration and increases at higher concentration is usually taken as an indication that intermolecular interactions occur between the pyrene pendants.³⁹ These intermolecular interactions promote the formation of intermolecular pyrene aggregates which constitute the cross-links of the Py–HASE network and lead to the viscosity increase observed in Figure 4. These results confirm qualitatively that a correlation exists between the pyrene associations, which occur at the molecular level, and the viscosity of the Py–HASE solution, which is a macroscopic property of the solution. A direct comparison of the variation of these parameters with the concentration of HASE35 is shown in Figure 6. To the best of our knowledge, it is only the second time that the molecular behavior of AP chains observed by fluorescence has been correlated qualitatively and directly with the viscosity of the aqueous solutions, with the first such study having been performed on a pyrene-labeled HEUR.⁴⁰

Another noticeable feature about the I_E/I_M ratio is that it increases linearly with pyrene concentration for Py–HASE concentrations above C^* , as expected for intermolecular excimer formation.²⁴ In the inset of Figure 5, the ratio $(I_E/I_M)/(I_E/I_M)_0$ is used to monitor the efficiency of a given Py–HASE sample at forming intermolecular excimer. To this effect, the I_E/I_M ratios

obtained for Py–HASEs at different concentrations were normalized by $(I_E/I_M)_0$, namely, the I_E/I_M ratio obtained at very low polymer concentration in the plateau region shown in the semilog plot of Figure 5. The straight lines intercepted the Y-axis at 1.0 and yielded slopes equal to 3.5, 1.1, and 0.8 for HASE12, HASE35, and HASE48, respectively. If the ratio $(I_E/I_M)_0$ is taken as a representation of intramolecular excimer formation, the difference $[(I_E/I_M) - (I_E/I_M)_0]$ represents intermolecular excimer formation. Thus, the ratio $[(I_E/I_M) - (I_E/I_M)_0]/(I_E/I_M)_0$ represents the increase of intermolecular excimer formation with respect to the intramolecular excimer formation. This quantity is proportional to $m \times [\text{Py}]$, where m is the slope of the straight lines shown in the inset of Figure 5.

On the basis of the values of the slopes reported above, it appears that, although the low pyrene content of HASE12 yields a small I_E/I_M ratio, HASE12 is much more efficient at forming intermolecular associations than HASE35 and HASE48 are. Since the efficiency of an AP solution at undergoing shear thinning depends on the ability of the AP to form intermolecular associations, the fluorescence results obtained with the Py–HASE samples should help rationalize their viscoelastic behavior. For instance, the shear-thinning effect of the 45 g/L Py–HASE solutions shown in Figure 2 is triggered by a much smaller shear rate for HASE35 ($0.8 \times 10^{-3} \text{ s}^{-1}$) and HASE48 ($0.3 \times 10^{-3} \text{ s}^{-1}$) than for HASE12 ($5 \times 10^{-3} \text{ s}^{-1}$). This result implies that more intermolecular associations need to be broken for HASE12 than for HASE35 and HASE48, in agreement with the trends obtained by fluorescence in the inset of Figure 5.

The other rather striking result of the inset of Figure 5 is that a linear increase of I_E/I_M with pyrene concentration is usually observed when the excimer is formed by diffusion.²⁴ However, this cannot be the case for the Py–HASE samples where about 58% of the pyrene pendants were found to be aggregated in aqueous solutions.²⁵ Consequently, it seems that the increase of Py–HASE concentration results in an increase of intermolecular interactions, as observed from the increase in the I_E/I_M ratio with excimer formation occurring by a combination of either diffusion or direct excitation of a ground-state pyrene aggregate. This result resembles that obtained with a Py–PEO model compound, where a linear increase of the I_E/I_M ratio with polymer concentration was observed in water, although the excimer did not exhibit any trace of a rise time.³²

An interesting feature of Figure 6 is that the I_E/I_M ratio increases while the macroscopic viscosity of the solution reaches values in the neighborhood of 1000 Pa·s. In the case of molecular pyrene dissolved in an organic solvent, such large viscosities would be expected to completely shut down the formation of excimer by diffusion so that the fraction of pyrenes which form excimer by diffusion should decrease. To check this hypothesis, time-resolved fluorescence decays of HASE35 and HASE48 were acquired for polymer concentrations ranging from 0.4 to 54 g/L in basic aqueous solutions (pH 9, 0.05 M KCl, 0.01 M Na₂CO₃). Despite the fact that the Py–HASEs studied in this section have pyrene contents slightly different from those studied in ref 25, their fluorescence decays were found to exhibit a very similar behavior. Within experimental error, all parameters retrieved from the analysis of the monomer and excimer fluorescence decays remained constant for a given polymer in aqueous solutions over the entire concentration range studied. They are listed in Supporting Information Tables SI.1–4. The values reported in this study are averaged over all polymer concentrations, and the listed errors represent the standard deviations calculated over all of the fluorescence decays acquired for a given polymer. The monomer and excimer decays

TABLE 3: Fractions f_{diff} , f_{free} , f_{E1} , and f_{E2} for HASE35 and HASE48 in Aqueous Solutions (pH 9, 0.05 M KCl, 0.01 M Na₂CO₃)

| sample | f_{diff} | f_{free} | f_{E1} | f_{E2} |
|--------|-------------------|-------------------|-----------------|-----------------|
| HASE35 | 0.23 ± 0.04 | 0.32 ± 0.05 | 0.38 ± 0.05 | 0.06 ± 0.01 |
| HASE48 | 0.28 ± 0.03 | 0.16 ± 0.04 | 0.52 ± 0.03 | 0.04 ± 0.01 |

were analyzed as described in ref 25 using sums of exponentials and the *blob* model.

The fractions of aggregated pyrenes, f_{agg} , for HASE35 and HASE48 in aqueous solutions (pH 9, 0.05 M KCl, 0.01 M Na₂CO₃) were determined according to an established protocol used to analyze the monomer and excimer fluorescence decays.^{25–31} As described earlier, four pyrene species are assumed to exist in solution. They are the pyrenes which are isolated in solution and cannot form excimer, $\text{Py}_{\text{free}}^*$, the pyrenes which form excimer via diffusion, $\text{Py}_{\text{diff}}^*$, the pyrenes which are aggregated and form an excimer instantaneously upon direct excitation, E1^* , and the pyrenes which are aggregated but do not adopt the proper geometry to form an excimer and emit with a long lifetime, E2^* . Analysis of the monomer and excimer fluorescence decays yields quantitative information about the concentrations of $\text{Py}_{\text{free}}^*$, $\text{Py}_{\text{diff}}^*$, E1^* , and E2^* at equilibrium, which is then used to determine a measure of the fractions of all pyrene species present in solution, namely, f_{free} , f_{diff} , f_{E1} , and f_{E2} , respectively. More information about the procedure used to determine f_{free} , f_{diff} , f_{E1} , and f_{E2} can be found in earlier publications.^{25–31} Their values are listed in Supporting Information Table SI.5. The values of f_{diff} , f_{free} , f_{E1} , and f_{E2} are constant over the whole range of Py–HASE concentrations, and their average values are reported in Table 3. The fraction of aggregated pyrenes, f_{agg} , equals the sum of f_{E1} and f_{E2} . It is shown as a function of polymer concentration in Figure 7. The f_{agg} values equal 0.44 ± 0.06 and 0.56 ± 0.03 for HASE35 and HASE48 in dilute aqueous solutions, respectively. Increasing the pyrene content of Py–HASE results in a modest increase in f_{agg} . This effect was not observed in ref 25 due to a stronger scattering of the data. As the pyrene content increases, f_{agg} increases (cf. Figure 7) at the expense of f_{free} (cf. Table 3). This result is expected because a higher pyrene content leads to fewer isolated pyrenes and stronger aggregation. These two effects rationalize the increase of the I_E/I_M ratio with increasing pyrene content observed in Figure 5.

Since f_{agg} remains constant above C_η in Figure 7, the occurrence of intermolecular associations between pyrene pendants for Py–HASE concentrations larger than $C^* \sim C_\eta$

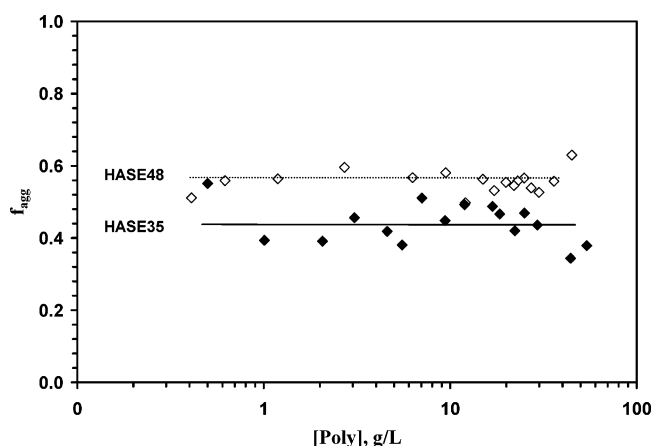


Figure 7. Fraction of associated pyrenes, f_{agg} , as a function of polymer concentration for HASE35 and HASE48 in basic aqueous solution (pH 9, 0.05 M KCl, 0.01 M Na₂CO₃).

(cf. Figure 5) is not accompanied by an increase of aggregation between the hydrophobes, contrary to what would be expected from the large increase in viscosity which should prevent excimer formation via diffusion and favor excimer emission from pyrene aggregates (cf. Figures 4 and 6). The reason for this result is certainly the fluidity experienced at the molecular level by the chains of an AP solution.² The macroscopic viscosity of the AP solution does not reflect the local mobility of the chains probed by time-resolved fluorescence at the molecular level which appears to be unaffected by the increase in Py–HASE concentration. Indeed, none of the parameters describing the time-dependent behavior of the pyrene pendants (f_{free} , f_{diff} , f_{E1} , and f_{E2} in Table 3 and Supporting Information Table SI.5) report any noticeable change with Py–HASE concentration. The increase of $I_{\text{E}}/I_{\text{M}}$ with increasing concentration above $C^* \sim C_{\eta}$ indicates that more intermolecular associations are occurring between the pyrene groups. Since all f_{free} , f_{diff} , f_{E1} , and f_{E2} fractions remain constant, it indicates that, above C^* , the contribution of pyrene associations occurring by diffusion and resulting in excimer formation does not change with respect to the contribution resulting from pyrene aggregation; only their overall numbers increase, resulting in the increase in $I_{\text{E}}/I_{\text{M}}$ with increasing concentration above $C^* \sim C_{\eta}$.

So far, only steady-shear viscosity measurements were used to characterize the viscoelastic properties of basic aqueous solutions of HASEs. In these experiments, the solutions are subject to large deformations. Dynamic rheological measurements are performed by applying small oscillatory deformations to the sample and are generally used to characterize the linear viscoelastic properties of melts, polymer solutions, and gels.⁴¹ The study of the viscoelastic properties of such polymeric systems yields information about their microstructure. Consequently, dynamic rheological measurements were performed on basic aqueous solutions of Py–HASEs and the effects of pyrene content and Py–HASE concentration on the solution viscoelastic properties were monitored. Figure 8 shows some representative profiles of the behavior of the complex viscosity, η^* , as a function of the angular frequency, ω , for aqueous solutions of Py–HASEs. No Newtonian plateau could be observed in the range of ω 's scanned for any of the Py–HASEs. This is a feature often encountered with HASEs^{7–9,14,21} and other APs with a structure similar to that of HASEs.¹⁶ Since a short Newtonian plateau was observed in the steady-shear viscosity profiles at very low shear rates (cf. Figures 2 and 3), the Newtonian plateau in the oscillatory measurements is expected to appear at lower ω values. Unfortunately, the Paar Physica DSR 4000 rheometer does not allow the reliable acquisition of data at ω 's lower than those used in this study.

Shear thinning was observed for all Py–HASEs. Figure 9 shows the effect of the pyrene content on η^* for aqueous solutions of the HASEs at 45 g/L. The trends observed for η^* are the same as those observed in Figure 2 for η . When shear thinning occurs, the slopes of the plots of $\log \eta^*$ versus $\log \omega$ are -0.42 , -0.77 , and -0.93 for HASE12, HASE35, and HASE48, respectively. Thus, the shear-thinning effect is more pronounced with HASEs having higher pyrene contents, a conclusion identical to that drawn from the steady-shear viscosity measurements (cf. Figure 2). For HASE0, η^* does not change much with ω . Only slight shear thinning is observed at values of ω higher than 2 rad/s.

The Cox–Merz rule is an empirical relationship which states that $\eta(\dot{\gamma})$ and $\eta^*(\omega)$ are superimposable for entangled polymeric systems such as melts and concentrated polymer solutions.⁴² This relationship is closely obeyed in aqueous solutions of

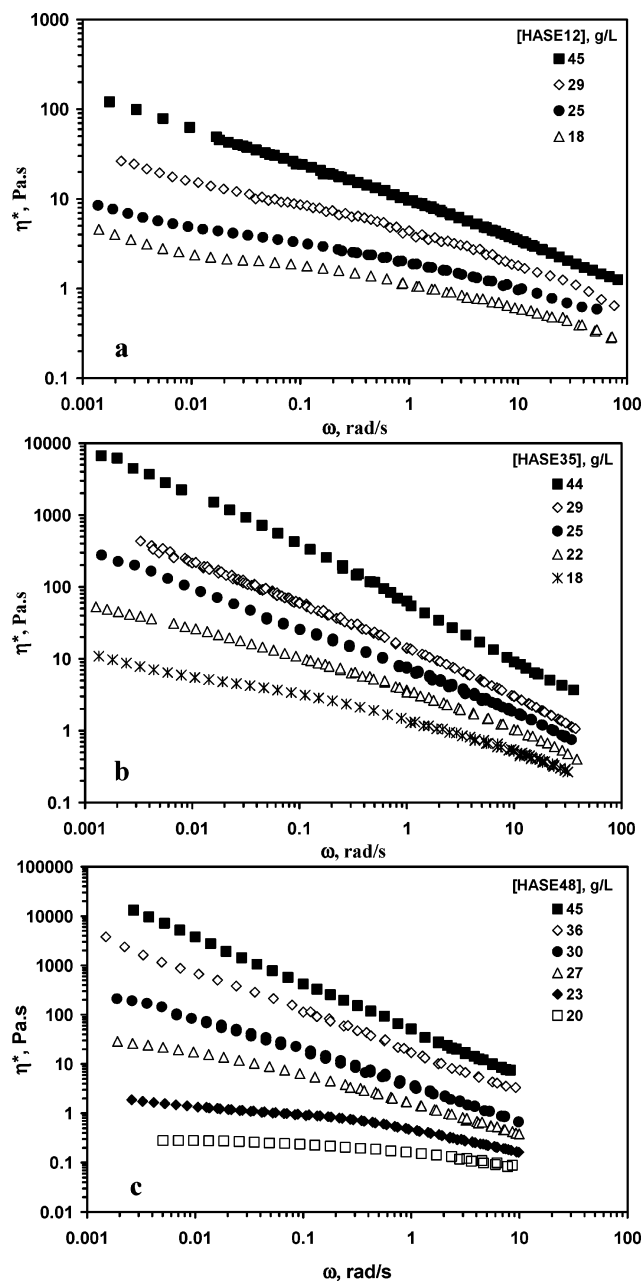


Figure 8. Effect of Py–HASE concentration on the complex viscosity, η^* , plotted as a function of angular frequency, ω , for Py–HASEs in basic aqueous solutions (pH 9, 0.05 M KCl, 0.01 M Na_2CO_3): HASE12 (a); HASE35 (b); HASE48 (c).

HASE0 at 45 g/L, as shown in Supporting Information Figure SI.1, and the viscosity of the Newtonian plateau is 0.89 ± 0.05 Pa·s. However, the Cox–Merz rule does not hold for the aqueous solutions of all Py–HASEs. As an example, the viscosity profiles of HASE48 at 45 g/L are given in Supporting Information Figure SI.1. $\eta^*(\omega)$ remains larger than $\eta(\dot{\gamma})$ over the entire range of ω 's and $\dot{\gamma}$ values studied, but $\eta^*(\omega)$ differs less from $\eta(\dot{\gamma})$ at a lower concentration of HASEs and/or pyrene contents (trends not shown). Here again, the nonconformity of Py–HASEs with the Cox–Merz rule has been observed with numerous other polymeric systems of multisticker chains.^{5,9,14}

The profiles of the storage, G' , and loss, G'' , moduli are routinely used to characterize the viscoelastic behavior of melts and concentrated polymer solutions because G' and G'' describe the elastic and viscous behavior of the fluid, respectively. For telechelic APs such as HEURs, the viscoelastic properties are

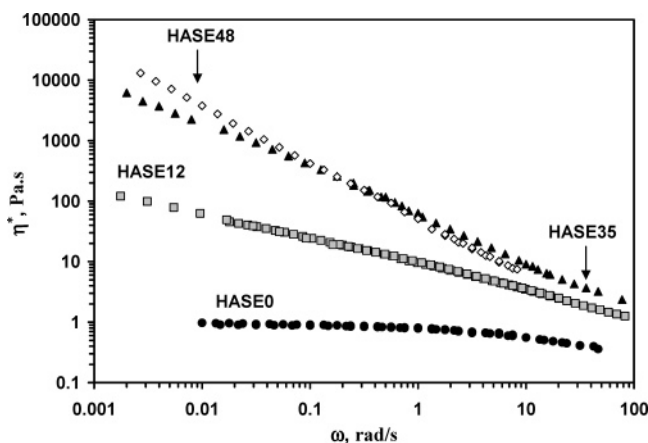


Figure 9. Effect of HASE concentration on the complex viscosity, η^* , plotted as a function of angular frequency, ω , for HASEs in basic aqueous solutions (pH 9, 0.05 M KCl, 0.01 M Na_2CO_3) at 45 g/L.

well defined by the Maxwell model with a single characteristic relaxation time which represents the residence time of a hydrophobe in an aggregate.³ At low ω 's, G' and G'' scale as ω^2 and ω^1 , respectively, a characteristic feature of Maxwellian fluids. Figures 10a, 10b, and 10c depict representative curves of the behavior of G' and G'' as a function of ω for HASE12, HASE35, and HASE48, respectively.

Figure 10 shows that, over a large frequency domain, G' and G'' increase as $G' \sim \omega^a$ and $G'' \sim \omega^b$, respectively. The values of a and b were determined and are listed in Supporting Information Table SI.6. The a values vary between 0.32 and 1.05, while the b values vary between 0.15 and 0.83. The viscoelastic behavior of the pyrene-labeled HASEs is clearly non-Maxwellian, as found with nonfluorescent HASEs.^{9,15} The a and b values decrease as the HASE concentration increases, becoming closer to zero at high HASE concentration, as expected for a gel-like behavior. The decrease in the values of a and b with concentration is slower for the HASE12 aqueous solutions than for the HASE35 and HASE48 aqueous solutions. Interestingly, the aqueous solution of HASE48 at 45 g/L exhibits the characteristic viscoelastic behavior of gels. The values of G' and G'' vary little with ω , and G' is always higher than G'' . This means that the elastic response of the sample dominates with respect to that of the viscous flow (cf. Supporting Information Figure SI.2). The complex viscosity of the 45 g/L HASE48 solution decreases linearly with angular frequency in a log-log plot with a slope of -0.93 , which is close to the -1.0 slope expected for gels.⁴³ Consequently, HASE48 at 45 g/L forms a physical gel in aqueous solutions through the association of the hydrophobic pyrenes.

The aqueous solutions of HASE48 at lower concentrations exhibit a behavior identical to that of the aqueous solutions of HASE35 (cf. Figure 10b,c). For these solutions, G' is lower than G'' at low ω values. Consequently, the viscous flow dominates over the elastic response. At higher ω 's, G' is larger than G'' in the range of ω 's scanned or would become larger if the profiles were extrapolated to ω values larger than those accessible with our instrument. At high ω 's, the elastic behavior of the sample predominates. At a certain angular frequency, ω_c , the G' and G'' traces intersect. This crossing point shifts to lower angular frequencies as the concentration of the solution increases. In the case of HASE12, a crossing point is observed for the 45 g/L solution at high ω values, while, for the other solutions, no crossing point is visible. Thus, the viscous flow dominates over the elastic behavior in the whole range of angular

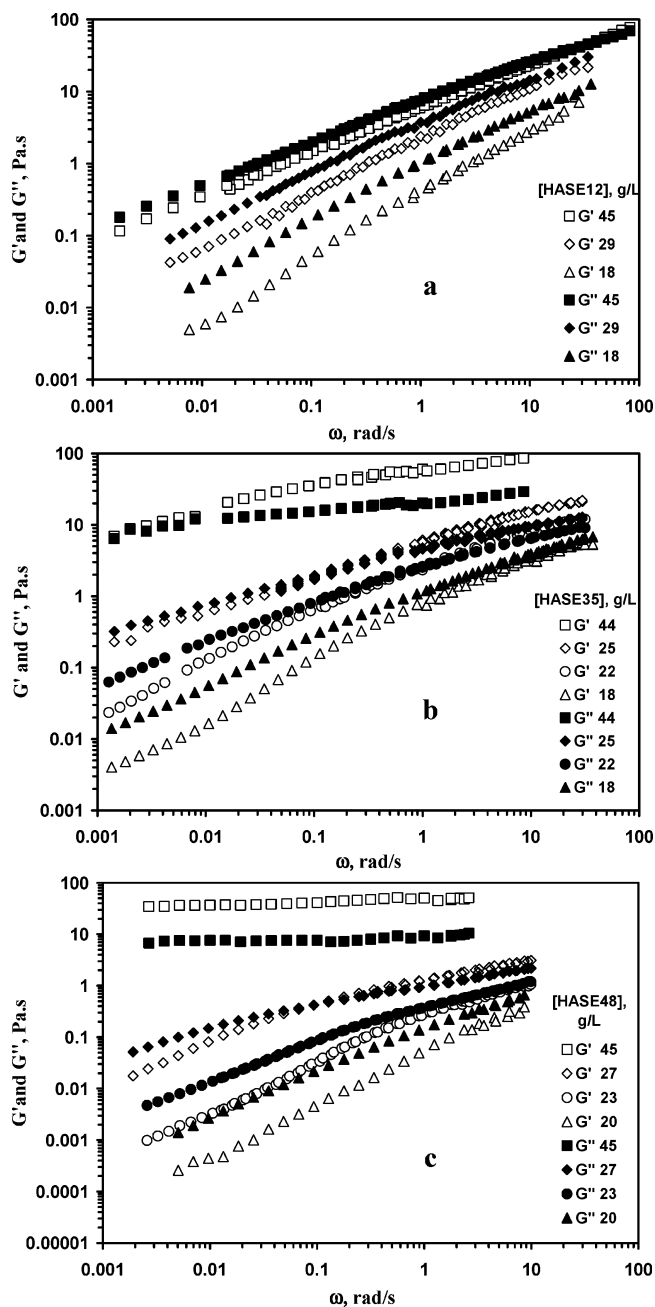


Figure 10. Representative profiles of storage (G' , empty symbols) and loss (G'' , filled symbols) moduli as a function of angular frequency for HASEs in basic aqueous solutions (pH 9, 0.05 M KCl, 0.01 M Na_2CO_3) at several HASE concentrations: HASE12 (a); HASE35 (b); HASE48 (c).

frequencies monitored (cf. Figure 10a). The increase of the elastic behavior with Py-HASE concentration observed for all Py-HASE samples is probably due to an increase of the density of intermolecular elastically active cross-linking centers. This statement is supported by the observed increase in the I_E/I_M ratio with Py-HASE concentration (cf. Figure 5).

The previous observations show that the Py-HASEs have very unusual and complicated viscoelastic properties, as observed by other researchers for nonfluorescent HASEs.^{7-9,14,15} These properties are due to the formation of a transient network held together by the hydrophobic associations of pyrenes which constitute the temporary cross-linking points of the network. The complicated viscoelastic properties of these systems can arise from the polydispersity of the polymeric chains and

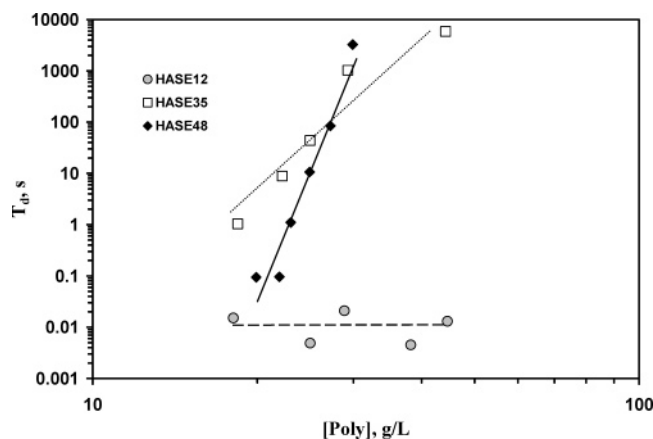


Figure 11. Concentration dependence of the terminal relaxation time, T_d , of basic aqueous solutions (pH 9, 0.05 M KCl, 0.01 M Na_2CO_3) of HASEs.

aggregate sizes, but more certainly from the peculiar comblike structure of HASEs.¹³

Discussion

Green and Tobolsky have developed a simple theory for the relaxation process of transient networks.⁴⁴ Transient networks which obey the Green and Tobolsky theory are described as having a Maxwellian behavior. This theory uses two fundamental parameters which are the high frequency plateau modulus, G_0 , and the terminal relaxation time, T_d . T_d is the reciprocal of ω_c which is the frequency where G' and G'' cross over, whereas G_0 is the limit of the storage modulus obtained at high frequency. This theory also predicts that $\eta_0 = T_d \times G_0$. As described in the Results section, the viscoelastic behavior of Py-HASEs is not Maxwellian. Consequently, the rheological data are much more difficult to analyze. However, protocols have been worked out to determine whether the relationship $\eta_0 = T_d \times G_0$ is obeyed even for APs which do not follow the Green and Tobolsky theory. In particular, such a protocol has been applied by Noda et al. to study the viscoelastic behavior of an AP whose structure is similar to that of HASEs.¹⁶ In the following discussion, we investigate whether this protocol is applicable to Py-HASEs.

In the Noda et al. protocol, the terminal relaxation time is assumed to be the point at which G' and G'' intersect.¹⁶ The crossing point is described by the frequency ω_c and the modulus G_c , where ω_c is the frequency at which $G' = G'' (=G_c)$. The values of ω_c and G_c are listed in Supporting Information Table SI.7. When G' and G'' would not intercept over the range of ω 's accessible with the rheometer, the intercept was estimated by extrapolating the trends of G' and G'' using linear approximations. The terminal relaxation times for the aqueous solutions of Py-HASEs were estimated using the relationship $T_d = 2\pi\omega_c^{-1}$, and the values are listed in Supporting Information Table SI.7 and plotted as a function of HASE concentration in Figure 11. For aqueous solutions of HASE12, T_d is essentially independent of polymer concentration and equals 0.012 ± 0.007 s. On the other hand, T_d increases with polymer concentration as C^x , where x equals 10 ± 1 and 27 ± 2 for aqueous solutions of HASE35 and HASE48, respectively. Such a power-law increase of T_d with polymer concentration has also been observed with other multisticker chains,¹⁶ but the exponent took smaller values of 7 and 9. It must be noted however that the range of concentrations over which these measurements are performed is rather narrow (less than 1 order of magnitude, cf.

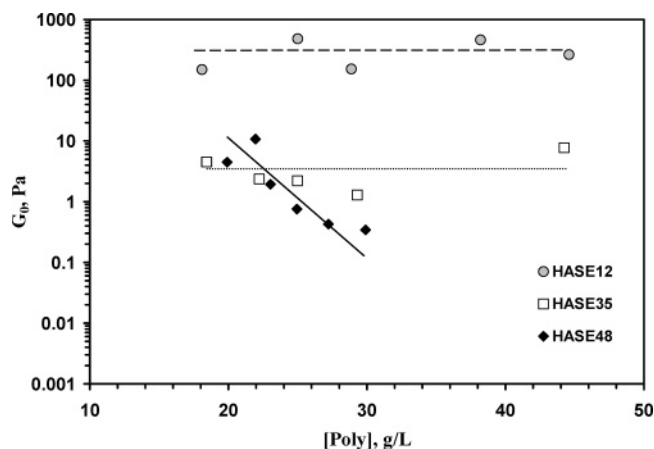


Figure 12. Concentration dependence of the high frequency plateau modulus, G_0 , of basic aqueous solutions (pH 9, 0.05 M KCl, 0.01 M Na_2CO_3) of pyrene-labeled HASEs.

Figure 11) which suggests that the error bars on the power-law exponents must have even larger uncertainties than those reported here.

Regardless of the exponent value, T_d values for HASE12 solutions are always lower in the entire range of concentrations studied than those for the other Py-HASEs. This observation indicates that the disruption of the network formed by the Py-HASEs in aqueous solutions depends strongly on pyrene content, that is, the density of hydrophobes in the polymer coil. At low pyrene contents, the Py-HASE concentration does not affect the lifetime of the transient network, while, at higher pyrene contents, the Py-HASE concentration represents a key parameter for the longest relaxation time of the transient network. Increasing the pyrene content of Py-HASEs results in a dramatic slowdown of the network dynamics at high polymer concentrations.

APs such as HEURs follow a Maxwellian behavior and have G' profiles which exhibit a plateau at high frequencies.³ The value of G' in this plateau region is referred to as G_0 . The G' profiles shown in Figure 10 do not display a clear plateau for the Py-HASEs in aqueous solution, as usually found for nonfluorescent HASEs.^{7–14} Consequently, G_0 for the slowest relaxation process is taken to equal G_c , the intersection of the extrapolated values of G' and G'' , as proposed by Noda et al.¹⁶ The estimated values for G_0 are listed in Supporting Information Table SI.7 and plotted in Figure 12. Within experimental error, the G_0 values for HASE12 and HASE35 remain nearly constant with concentration, taking average values of 305 ± 165 and 3.6 ± 2.6 Pa, respectively. G_0 decreases with concentration for HASE48 as C^x , where x equals -8 ± 2 . As for the C^x power laws obtained with T_d , the HASE48 concentrations range only from 20 to 30 g/L, a range too narrow to yield sufficient accuracy on the exponent of the power law. Nevertheless, the trends shown in Figure 12 indicate that the G_0 values for HASE48 become smaller than the G_0 values for HASE35, as the HASE concentration increases. The theory of Green and Tobolsky⁴⁴ suggests that G_0 is proportional to the number density of elastically active chains, ν , according to the relationship $G_0 = \nu k_B T$, where k_B is the Boltzmann constant and T is the absolute temperature. This relationship and the data shown in Figure 12 imply that the number density of elastically active chains decreases with increasing pyrene content of the Py-HASE sample. This is a rather surprising conclusion because one would intuitively expect the elastic behavior of HASE48 solutions to arise from a larger density of elastically active

chains. Nevertheless, the following explanation can be proposed. A Py-HASE with a lower pyrene content has a lower density of pyrenes per coil. Since intramolecular hydrophobic associations have been shown to contract the overall coil dimensions of an AP,^{35,36} the coils of HASE12 are expected to be less compact than those of HASE35 and HASE48. Consequently, HASE12 is more inclined to generate intermolecular associations than HASE35 or HASE48 are. As a result, the Py-HASEs with lower pyrene content generate more elastically active chains between aggregates, that is, a larger number of elastically active chains than Py-HASEs with higher pyrene contents do. Interestingly, this reasoning is supported by the fluorescence results shown in the inset of Figure 5 where HASE12 was shown to be much more efficient at forming intermolecular associations than HASE35 and HASE48.

As mentioned earlier, the Green–Tobolsky theory predicts that $T_d \times G_0$ equals η_0 , as observed by Noda et al. for copolymers of sodium acrylate and methacrylates substituted with amphiphiles.¹⁶ Supporting Information Figures SI.3 and SI.4 show the plots of $T_d \times G_0$ and η_0 as a function of polymer concentration for HASE35 and HASE48, respectively. These plots indicate that the $T_d \times G_0$ products (obtained from oscillatory viscosity measurements) overlap very well with the η_0 values (obtained by steady-shear viscosity measurements). For HASE12, this prediction fails completely because η_0 increases with concentration (cf. Figure 4) while T_d and G_0 remain constant (cf. Figures 11 and 12, respectively). Since G_0 remains more or less constant with Py-HASE concentration for HASE35 and HASE48, the dramatic increase of η_0 with increasing Py-HASE concentration observed in Figure 4 is due essentially to the drastic lengthening of the terminal relaxation time, T_d , of the Py-HASE solution.

In summary, the viscoelastic properties of the Py-HASEs are unusual and complicated to interpret because they do not obey any existing models describing transient polymeric networks. In that respect, they do mimic the viscoelastic properties reported for numerous other nonfluorescent HASE systems.^{7–14} The viscoelastic behavior of Py-HASEs is not Maxwellian, since the moduli G' and G'' do not scale as ω^2 and ω^1 , respectively. The Cox–Merz rule is not obeyed. However, the product $T_d \times G_0$ and η_0 of HASE35 and HASE48 overlap nicely when plotted against concentration in Figures SI.3 and SI.4 in Supporting Information, indicating that, despite the approximations made in the Noda et al. protocol used to handle the dynamic viscosity data,¹⁶ the T_d and G_0 values of HASE35 and HASE48 must be fairly close to the genuine values.

The fluorescence and rheology measurements indicate that, above C^* , the Py-HASEs with low pyrene contents form more intermolecular associations (cf. Figures 5 and 12) and have a small terminal relaxation time (cf. Figure 11), whereas the Py-HASEs with high pyrene contents form less intermolecular associations but have a much slower terminal relaxation time. The picture that emerges is that Py-HASEs assemble into units (arbitrarily represented as circles in Figure 13) made of several Py-HASE chains whose internal rigidity is determined by the density of internal or “intraunit” hydrophobic aggregates. A large density of intraunit hydrophobic aggregates yields rigid units such as those of HASE35 and HASE48, whereas a small density of intraunit hydrophobic aggregates yields flexible units such as those of HASE12. Above C^* , each unit is connected to others via interunit hydrophobic aggregates. The density of interunit hydrophobic aggregates is large in the case of Py-HASEs having a low pyrene content like HASE12, but it is smaller in the case of Py-HASEs having a high pyrene content like

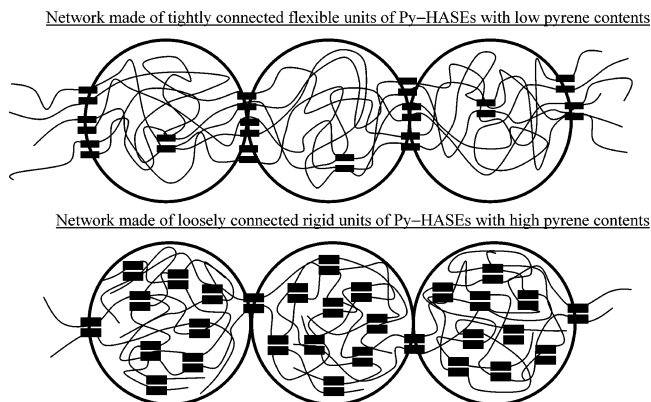


Figure 13. Schematic representation of a network made of Py-HASE circular units held by hydrophobic aggregates. The top and bottom panels represent Py-HASEs having a low and high pyrene content, respectively.

HASE35 and HASE48. Under shear, Py-HASEs with low pyrene contents will require a larger shear rate to disrupt the numerous interunit hydrophobic aggregates (cf. Figure 2) and their G_0 (cf. Figure 12) and $[(I_E/I_M) - (I_E/I_M)_0]/(I_E/I_M)_0$ (cf. inset of Figure 5) values are large. However, because they exhibit less intraunit hydrophobic aggregates, they exhibit internal flexibility. Thus, the chains inside a unit are relatively mobile which allows a rapid rearrangement of the disrupted hydrophobes under shear. Their terminal relaxation time is small (cf. Figure 11). Py-HASEs with high pyrene contents will form less interunit hydrophobic associations and their G_0 (cf. Figure 12) and $[(I_E/I_M) - (I_E/I_M)_0]/(I_E/I_M)_0$ (cf. inset of Figure 5) values are small. Consequently, a smaller shear rate is necessary to break up the fewer interunit aggregates and induce shear thinning, as shown in Figure 2. However, their large number of intraunit hydrophobic aggregates confer them an internal rigidity which reduces the mobility of the chains inside a unit and hinders the rapid rearrangement of the hydrophobic pendants when the solution is under shear. As a result, they exhibit large terminal relaxation times (cf. Figure 11). The qualitative description proposed above for the viscoelastic behavior of Py-HASEs has been summarized in Figure 13.

In Figure 13, increasing the Py-HASE concentration above C^* generates more intermolecular interactions between the pyrene pendants and the I_E/I_M ratio increases (cf. Figure 5). These intermolecular associations occur mostly inside a unit via both diffusional encounters between pyrene pendants and formation of ground-state pyrene aggregates, as demonstrated by time-resolved fluorescence measurements (cf. Figure 7). Above C^* , the density of ground-state pyrene aggregates inside the units increases with increasing polymer concentration which results in an increase of the intraunit rigidity and an increase of T_d (cf. Figure 11). Because the intermolecular associations occur mostly inside one unit, the density of elastically active junctions between units is not affected and G_0 remains constant (cf. Figure 12).

Conclusions

Basic aqueous solutions of Py-HASEs were characterized by fluorescence and rheology measurements. Using these two techniques, a correlation was shown to exist between the formation of hydrophobic associations taking place at the molecular level among the pyrene pendants and the increase of the macroscopic viscosity of the Py-HASE aqueous solutions. The increase in the values of the I_E/I_M ratio with HASE concentration is accompanied by a dramatic increase of the

solution viscosity. The trends shown by the I_E/I_M ratio indicate that the Py–HASE sample with the smallest pyrene content is much more efficient at forming intermolecular associations than the Py–HASE samples having a higher pyrene content, a conclusion in agreement with the results obtained from the viscoelastic measurements. The time-resolved fluorescence measurements demonstrated that the local mobility of the polymer chains seems to be unaffected by the large increase of the macroscopic viscosity of the solution.

In addition to steady flow, dynamic rheological measurements were used to probe the rheological behavior of the Py–HASEs in aqueous solution. The results show that concentration and pyrene content have a dramatic effect on the linear viscoelastic properties of the solution and consequently on the relaxation of the polymer coils. The coils of HASE35 and HASE48 have a high density of hydrophobic groups. When the polymer concentration increases, more intermolecular hydrophobic associations are formed which delay the motion of the polymeric chain, giving rise to a strong dependence of T_d on polymer concentration. The plateau modulus, G_0 , was found to remain constant with HASE concentration for HASE12 and HASE35 and to decrease for HASE48. Surprisingly, G_0 decreases with increasing pyrene content. This result indicates that HASE12 has the highest number of elastically active chains and HASE48 has the lowest. This effect is due to the greater ability of HASE12 at promoting interpolymeric associations, as shown by fluorescence measurements.

More importantly, the bulk of these results demonstrates that the incorporation of the aromatic hydrophobe pyrene into HASEs results in a rheological behavior which is similar to that observed with nonfluorescent HASEs. Thus, this confirms the validity of using Py–HASEs as fluorescent model compounds to improve our basic understanding of AP solutions. The combination of fluorescence measurements which provide information on the hydrophobes of an AP at the molecular level with rheology experiments which provide information about the macroscopic viscoelastic properties of an AP solution should help rationalize the structure–property relationship of AP solutions.

Supporting Information Available: Tables showing the parameters retrieved from the triexponential fit and the fit (with the blob model equations²⁵) of the pyrene monomer and excimer fluorescence decays of the HASE polymers; fractions of $[Py^*_{free}]_{(t=0)}$, $[Py^*_{diff}]_{(t=0)}$, $[E1^*]_{(t=0)}$, and $[E2^*]_{(t=0)}$ for HASEs; values of a and b ; and estimated values of ω_c , T_d , G_c , and G_0 and figures showing a comparison of the steady-shear viscosity and the complex viscosity as a function of shear rate and angular frequency; a plot of the complex viscosity, storage modulus, and loss modulus as a function of angular frequency (for HASE48 at 45 g/L); and plots of the concentration dependence of η_0 and the product $T_d \times G_0$. This material is available free of charge via the Internet at <http://pubs.acs.org>.

References and Notes

- (1) Winnik, M. A.; Yekta, A. *Curr. Opin. Colloid Interface Sci.* **1997**, *2*, 424–436.
- (2) Tanaka, F.; Edwards, S. F. *J. Non-Newtonian Fluid Mech.* **1992**, *43*, 247–271.
- (3) Annable, T.; Buscall, R.; Ettelaie, R.; Whittlestone, D. *J. Rheol.* **1993**, *37*, 695–725.
- (4) Annable, T.; Buscall, R.; Ettelaie, R. *Colloids Surf., A* **1996**, *112*, 97–116.
- (5) Regalado, E. J.; Selb, J.; Candau, F. *Macromolecules* **1999**, *32*, 8580–8588.
- (6) Candau, F.; Regalado, E. J.; Selb, J. *Macromolecules* **1998**, *31*, 5550–5552.
- (7) Tirtaatmadja, V.; Tam, K. C.; Jenkins, R. D. *Macromolecules* **1997**, *30*, 1426–1433.
- (8) Tirtaatmadja, V.; Tam, K. C.; Jenkins, R. D. *Macromolecules* **1997**, *30*, 3271–3282.
- (9) English, R. J.; Gulati, H. S.; Jenkins, R. D.; Khan, S. A. *J. Rheol.* **1997**, *41*, 427–444.
- (10) Tam, K. C.; Farmer, M. L.; Jenkins, R. D.; Bassett, D. R. *J. Polym. Sci., Part B: Polym. Phys.* **1998**, *36*, 2275–2290.
- (11) Tam, K. C.; Guo, L.; Jenkins, R. D.; Bassett, D. R. *Polymer* **1999**, *40*, 6369–6379.
- (12) Tan, H.; Tam, K. C.; Tirtaatmadja, V.; Jenkins, R. D.; Bassett, D. R. *J. Non-Newtonian Fluid Mech.* **2000**, *92*, 167–185.
- (13) Jenkins, R. D.; DeLong, L. M.; Bassett, D. R. In *Hydrophobic Polymers. Performance with Environmental Acceptability*; Glass, J. E., Ed.; Advances in Chemistry Series 248; American Chemical Society: Washington, DC, 1996; pp 425–447.
- (14) Pellens, L.; Corrales, R. G.; Mewis, J. *J. Rheol.* **2004**, *48*, 379–393.
- (15) Mewis, J.; Kaffashi, B.; Vermant, J.; Butera, R. J. *Macromolecules* **2001**, *34*, 1376–1383.
- (16) Noda, T.; Hashidzume, A.; Morishima, Y. *Langmuir* **2001**, *17*, 5984–5991.
- (17) Noda, T.; Hashidzume, A.; Morishima, Y. *Macromolecules* **2001**, *34*, 1308–1317.
- (18) Noda, T.; Hashidzume, A.; Morishima, Y. *Polymer* **2001**, *42*, 9243–9252.
- (19) Leibler, L.; Rubinstein, M.; Colby, R. H. *Macromolecules* **1991**, *24*, 4701–4707.
- (20) de Gennes, P.-G. *Scaling Concepts in Polymer Physics*; Cornell University Press: Ithaca, NY, 1979; p 226.
- (21) Abdala, A. A.; Olesen, K.; Khan, S. A. *J. Rheol.* **2003**, *47*, 497–511.
- (22) Winnik, F. M. *Chem. Rev.* **1993**, *93*, 587–614.
- (23) Duhamel, J. In *Molecular Interfacial Phenomena of Polymer and Biopolymers*; Chen, P., Ed.; Woodhead: New York, 2005.
- (24) Birks, J. B. *Photophysics of Aromatic Molecules*; Wiley: New York, 1970; p 351.
- (25) Prazeres, T. J. V.; Beingessner, R.; Duhamel, J.; Olesen, K.; Shay, G.; Bassett, D. R. *Macromolecules* **2001**, *34*, 7876–7884.
- (26) Siu, H.; Duhamel, J. *J. Phys. Chem. B* **2005**, *109*, 1770–1780.
- (27) Siu, H.; Duhamel, J. *Macromolecules* **2004**, *37*, 9287–9289.
- (28) Kanagalingam, S.; Ngan, C. F.; Duhamel, J. *Macromolecules* **2002**, *35*, 8560–8570.
- (29) Duhamel, J.; Kanagalingam, S.; O'Brien, T.; Ingratta, M. *J. Am. Chem. Soc.* **2003**, *125*, 12810–12822.
- (30) Zhang, M.; Duhamel, J.; van Duin, M.; Meessen, P. *Macromolecules* **2004**, *37*, 1877–1890.
- (31) Picarra, S.; Duhamel, J.; Fedorov, A.; Martinho, J. M. G. *J. Phys. Chem. B* **2004**, *108*, 12009–12015.
- (32) Siu, H.; Prazeres, T. J. V.; Duhamel, J.; Olesen, K.; Shay, G. *Macromolecules* **2005**, *38*, 2865–2875.
- (33) Islam, M. F.; Jenkins, R. D.; Bassett, D. R.; Lau, W.; Ou-Yang, H. D. *Macromolecules* **2000**, *33*, 2480–2485.
- (34) Tirtaatmadja, V.; Tam, K. C.; Jenkins, R. D.; Bassett, D. R. *Colloid Polym. Sci.* **1999**, *277*, 276–281.
- (35) Volpert, E.; Selb, J.; Candau, F. *Macromolecules* **1996**, *29*, 1452–1463.
- (36) Guo, L.; Tam, K. C.; Jenkins, R. D.; *Macromol. Chem. Phys.* **1998**, *199*, 1175–1184.
- (37) Seng, W. P.; Tam, K. C.; Jenkins, R. D.; Bassett, D. R. *Macromolecules* **2000**, *33*, 1727–1733.
- (38) Dai, S.; Tam, K. C.; Jenkins, R. D.; Bassett, D. R. *Macromolecules* **2000**, *33*, 7021–7028.
- (39) Kim, S. D.; Torkelson, J. M. *Macromolecules* **2002**, *35*, 5943–5952.
- (40) Richey, B.; Kirk, A. B.; Eisenhart, E. K.; Fitzwater, S.; Hook, J. J. *Coat. Technol.* **1991**, *63*, 31–40.
- (41) Ferry, J. D. *Viscoelastic Properties of Polymers*; John Wiley and Sons: New York, 1980; pp 108–109.
- (42) Cox, W. P.; Merz, E. H. *J. Polym. Sci.* **1958**, *28*, 619–622.
- (43) See, for example: Morris, E. R. In *The structure, Dynamics and Equilibrium of Colloidal Systems*; Bloor, D. M., Wyn-Jones, E., Eds.; Kluwer Academic Publishers: 1990; pp 449–470. Clark, A. H.; Ross-Murphy, S. B. *Adv. Polym. Sci.* **1987**, *83*, 57–192.
- (44) Green, M. S.; Tobolsky, A. V. *J. Chem. Phys.* **1946**, *14*, 80–92.